Extreme value statistics of ergodic Markov processes from first passage times in the large deviation limit

OPEN ACCESS
IOP Publishing
Journal of Physics A: Mathematical and Theoretical
J. Phys. A: Math. Theor. **52** (2019) 244001 (17pp)
https://doi.org/10.1088/1751-8121/ab1eca

Extreme value statistics of ergodic Markov processes from first passage times in the large deviation limit

David Hartich and Aljaž Godec[1]

Mathematical Biophysics Group, Max-Planck-Institute for Biophysical Chemistry, Göttingen 37077, Germany

E-mail: david.hartich@mpibpc.mpg.de and agodec@mpibpc.mpg.de

Received 29 January 2019, revised 8 April 2019
Accepted for publication 2 May 2019
Published 21 May 2019

Abstract

Extreme value functionals of stochastic processes are inverse functionals of the first passage time—a connection that renders their probability distribution functions equivalent. Here, we deepen this link and establish a framework for analyzing extreme value statistics of ergodic reversible Markov processes in confining potentials on the hand of the underlying relaxation eigenspectra. We derive a chain of inequalities, which bounds the long-time asymptotics of first passage densities, and thereby extrema, from above and from below. The bounds involve a time integral of the transition probability density describing the relaxation towards equilibrium. We apply our general results to the analysis of extreme value statistics at long times in the case of Ornstein–Uhlenbeck process and a 3D Brownian motion confined to a sphere, also known as Bessel process. We find that even on time-scales that are shorter than the equilibration time, the large deviation limit characterizing long-time asymptotics can approximate the statistics of extreme values remarkably well. Our findings provide a novel perspective on the study of extrema beyond the established limit theorems for sequences of independent random variables and for asymmetric diffusion processes beyond a constant drift.

Keywords: first passage time, record statistics, extreme value theory, Markov processes, Fokker–Planck equation, large deviation theory, eigenspectrum

(Some figures may appear in colour only in the online journal)

[1] Author to whom any correspondence should be addressed.

1. Introduction

The statistical properties of extreme values, which correspond to record-breaking events of a stochastic process, attracted increasing interest in various fields of research over the past decades. For example, climate changes were found to be reflected in the appearance of extreme (record-breaking) temperatures [1, 2], rainfall [3, 4], and possibly other extreme weather conditions [5]. Statistics of records are also important in the context of earthquakes [6], in studies of stock pricing in economics [7, 8], sports [9, 10], and in the theory of random matrices [11–13] to name but a few (see, e.g. [14, 15] for a more detailed overview).

In sequences of independent random variables extreme values approach one of the three classes of limiting distributions, which are denoted by the Gumbel [16], Fréchet, and Weibull distributions (see, e.g. [14, 17–20]). However, as soon as consecutive time steps of a stochastic process become correlated, a theoretical discussion of the statistics of extrema becomes more challenging [21]. In this case universal laws have been discovered, for example, for processes with symmetric step-length distributions [22, 23]. Subsequent studies also investigated correlations between records [24, 25] as well as their persistence [26–28] and number [29], and extensions have been made to processes with constant drift [27, 30–32] (see also [33] for an interesting experiment with trapped Cs atoms). A recent physical application includes the observation that the mean value of the minimum of the entropy production in stationary driven systems is bounded by the negative value of Boltzmann's constant '$-k_{\mathrm{B}}$' [34], which is also confirmed by experiments [35].

More broadly, a deep and important connection has been established, relating the statistics of extreme values to first passage times [14, 23, 36, 37]. In this work we deepen this connection between the first passage and the extremum functional, which allows us to obtain the statistics of extreme values in finite time for Markovian diffusion processes in confining potentials on time-scales, where consecutive time-steps remain correlated. Exploiting further a duality between first passage processes and ensemble propagation [38, 39] we derive a chain of inequalities, which bound the long time asymptotics (i.e. the large deviation limit) of the probability densities of extrema both from above and from below. As we will show, the large deviation limit approximates the probability density of extreme values surprisingly well even on relatively short time-scales.

The paper is organized as follows. In section 2 we recapitulate the well-known connection between distributions of extrema and first passage time densities. We then utilize recent findings on the large time asymptotics of first passage time densities [38, 39] to determine distributions of extrema in the large deviation limit. The usefulness of our general results is demonstrated in section 3, by determining the long-time statistics of maxima of the Ornstein–Uhlenbeck process and the statistics of the minimum of the 3D Brownian motion (Bessel process) confined to a sphere. All analytical results are corroborated by Brownian dynamics simulations. We conclude in section 4.

2. Fundamentals

2.1. Extreme values from first passage times

We consider processes governed by an overdamped Langevin equation

$$\dot{x}_t = -\beta D U'(x_t) + \xi_t \tag{1}$$

where $U'(x) = \partial_x U(x)$ is the gradient of a potential $U(x)$ and ξ_t stands for Gaussian white noise with zero mean and covariance $\langle \xi_t \xi_{t'} \rangle = 2D\delta(t - t')$. Without any loss of generality

we set the inverse temperature β and diffusion coefficient D to unity ($\beta \equiv D \equiv 1$), i.e. free energies U are expressed in units of $k_{\mathrm{B}}T$. The Fokker–Planck equation corresponding to the Langevin equation (1) reads [40]

$$\partial_t P(x,t|x_0) = \partial_x\big[\partial_x + U'(x)\big]P(x,t|x_0) \equiv \mathcal{L}_{\mathrm{FP}}P(x,t|x_0), \tag{2}$$

where $P(x,t|x_0) = \langle\delta(x - x_t)\rangle$ is the normalized probability density for a particle starting from x_0 to be found at position $x_t = x$ at time t with the initial condition $P(x,0|x_0) = \delta(x - x_0)$. The probability density function relaxes to the normalized Boltzmann–Gibbs equilibrium density $P^{\mathrm{eq}}(x) \equiv P(x,\infty|x_0) \propto \mathrm{e}^{-U(x)}$ for any x_0, which requires a sufficiently confining potential $U(x)$.

While the probability density $P(x,t|x_0)$ only depends on the initial and final states, the extreme values are functionals that depend on the entire history along a trajectory $\{x_\tau\}_{0\leqslant\tau\leqslant t}$. We define the maximum and the minimum of the process x_t as

$$\overline{m}_t \equiv \max_{0\leqslant\tau\leqslant t}(x_\tau) \qquad \text{and} \qquad \underline{m}_t \equiv \min_{0\leqslant\tau\leqslant t}(x_\tau), \tag{3}$$

respectively. For a given initial condition x_0 the extrema satisfy $\overline{m}_t \geqslant x_0$ as well as $\underline{m}_t \leqslant x_0$, where $\overline{m}_t$ is non-decreasing and $\underline{m}_t$ non-increasing in time t (see figure 1). It can be shown that the first passage time defined as

$$t_a(x_0) \equiv \min_{\tau\geqslant 0}(\tau|x_\tau = a) \tag{4}$$

is an inverse functional of the extrema. To see that we consider the distribution function of the maximum of the process $\overline{m}_t = \max_{0\leqslant\tau\leqslant t}(x_\tau)$, i.e. the probability that $\overline{m}_t$ exceeds the value $a \geqslant x_0$, $P^{\max}(a|t,x_0)$, which satisfies

$$P^{\max}(a|t,x_0) \equiv \mathrm{Prob}\,[a > \overline{m}_t] = \mathrm{Prob}\,[t_a(x_0) > t] \equiv \mathcal{P}_a(t|x_0), \tag{5}$$

where $\mathcal{P}_a(t|x_0)$ is called the survival probability (see also figure 1(a)). Equation (5) can be interpreted as follows: each path, whose maximum $\overline{m}_t$ after time t is smaller than a, must have a first passage time from x_0 to $a \geqslant x_0$, $t_a(x_0)$, larger than t. Equation (5) connects the first passage time functional $t_a(x_0)$ (where time is stochastic and position is fixed to a) to the maximum value functional $\overline{m}_t$ (where time is fixed to t and the position is stochastic). Note that the survival probability can also be expressed as the integral over the first passage time density $\wp_a$ via

$$\mathcal{P}_a(t|x_0) = \int_t^\infty \wp_a(\tau|x_0)\mathrm{d}\tau, \tag{6}$$

i.e. $\wp_a(\tau|x_0) = -\partial_t\mathcal{P}_a(t|x_0)$.

The minimum of a process $\underline{m}_t = \min_{0\leqslant\tau\leqslant t} x_t$ can be studied in a similar manner as the maximum, since $\underline{m}_t$ is equivalent to the maximum of the reflected process $-x_\tau$, i.e. $\underline{m}_t = -\max_{0\leqslant\tau\leqslant t}(-x_\tau)$. Hence, in the case of the minimum ($a \leqslant x_0$) equation (5) holds with the replacement $P^{\min}(a|t,x_0) = \mathrm{Prob}\,[a < \underline{m}_t] = \mathcal{P}_a(t|x_0)$, which is illustrated in figure 1(b). For convenience, we simply refer to P^κ as the extremum distribution function, which in the case $x_0 \leqslant a$ corresponds to the maximum distribution ($\kappa = \max$) and for $x_0 \geqslant a$ to the minimum distribution ($\kappa = \min$). The density of the extremum ($\kappa = \max, \min$) in either case is then given by the slope of the distribution function

$$p^\kappa(a|t,x_0) = \big|\partial_a P^\kappa(a|t,x_0)\big| = \big|\partial_a\mathcal{P}_a(t|x_0)\big|, \tag{7}$$

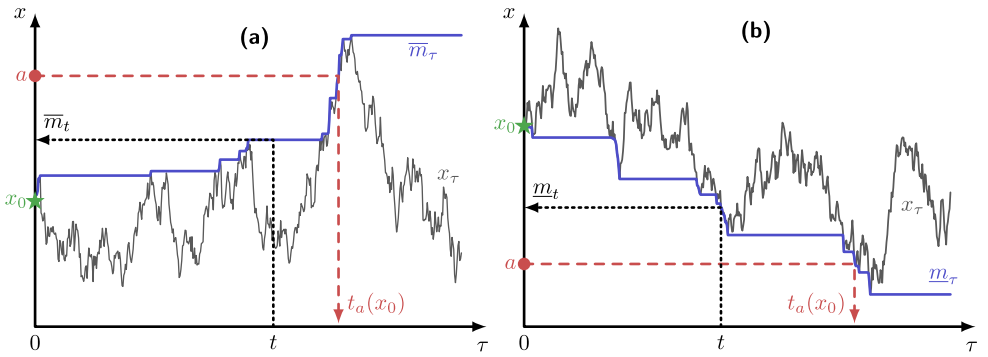

Figure 1. Schematics of the extreme value functional versus first passage time functional for a process $\{x_\tau\}_{0\leqslant\tau}$. (a) Schematics of the maximum functional $\overline{m}_\tau$ (thick blue line) of the process x_τ (thin gray line) as function of time τ; the dotted black arrow indicates the functional of the maximum $\overline{m}_t$ and the dashed red arrow represents first passage time $t_a(x_0)$; the arrows indicate the equivalence between $a > \overline{m}_t$ and $t_a(x_0) > t$. (b) The minimum functional $\underline{m}_\tau$ (thick blue line) defined analogously to (a), whereas $a < \underline{m}_t$ is here equivalent to $t_a(x_0) > t$.

where in the second step we used equation (5). Equation (7) describes the density of maxima ($\kappa = \max$) for $a \geqslant x_0$ and the density of the minima ($\kappa = \min$) for $a \leqslant x_0$. For example, the mean value of the maximum and minimum are given, respectively, by

$$\begin{aligned}\langle \overline{m}_t\rangle &= \int_{x_0}^{\infty} p^{\max}(a|t,x_0)a\mathrm{d}a = x_0 + \int_{x_0}^{\infty} \mathcal{P}_a(t|x_0)\mathrm{d}a,\\ \langle \underline{m}_t\rangle &= \int_{-\infty}^{x_0} p^{\min}(a|t,x_0)a\mathrm{d}a = x_0 - \int_{-\infty}^{x_0} \mathcal{P}_a(t|x_0)\mathrm{d}a,\end{aligned} \tag{8}$$

where we used equation (7) and performed a partial integration in the last step in both lines.

In the following subsection we focus on the probability density function of the two extrema $p^{\max}$ and $p^{\min}$, whereas further discussions on the mean of extreme value fluctuations ($\langle \underline{m}_t\rangle$ or $\langle \overline{m}_t\rangle$) can be found, for example, in [21, 23–25, 41]. Notably, $t_a(x_0)$—the first passage time from x_0 to $a \geqslant x_0$—is unaffected by the potential landscape $U(x)$ beyond $x \geqslant a$, which according to equation (5) implies that any two potentials $U_1(x), U_2(x)$ with $U_1(x) = U_2(x)$ for all $x \leqslant R$ generate the same maximum distribution $P^{\max}$ for all $a \leqslant R$.

2.2. First passage time statistics from ensemble propagation

According to equation (5) the problem of determining the statistics of the extremum $P^{\max}(a|t,x_0)$ is in fact equivalent to determining the survival probability $\mathcal{P}_a(t|x_0)$, or, according to equation (6), to determining the first passage time density $\wp_a(t|x_0) = -\partial_t \mathcal{P}_a(t|x_0)$, which will be the central goal of this section.

We determine the first passage time density (or survival probability) using the renewal theorem [42]

$$P(a,t|x_0) = \int_0^t P(a,t-\tau|a)\wp_a(\tau|x_0)\mathrm{d}\tau, \tag{9}$$

reflecting the fact that all the paths starting from x_0 and ending up in a after time t by construction must reach a for the first time at some time $\tau \leqslant t$, and then return to a again after time

$t-\tau$. We have recently established a duality between first passage and relaxation processes, i.e. between P and $\wp_a$, which will allow us to solve equation (9) for $\wp_a$ in the following manner (see also [38, 39] for more details).

First, we Laplace-transform[2] the renewal theorem (9) in time ($t \to s$), which converts the convolution to a product, $\tilde{P}(a,s|x_0) = \tilde{P}(a,s|a)\tilde{\wp}_a(s|x_0)$, implying

$$\tilde{\wp}_a(s|x_0) = \frac{\tilde{P}(a,s|x_0)}{\tilde{P}(a,s|a)}, \tag{10}$$

where $\tilde{\wp}_a(s|x_0)$ is the Laplace transform of the first passage time density and $\tilde{P}(x,s|x_0)$ obeys the Laplace transformed Fokker–Planck equation (2)

$$[\mathcal{L}_{\mathrm{FP}} - s]\tilde{P}(x,s|x_0) = -\delta(x-x_0) \tag{11}$$

with natural boundary conditions. The next step is to render equation (10) explicit in the time domain, i.e. to find the explicit inverse Laplace transform $\tilde{\wp}_a(s|x_0) \to \wp_a(t|x_0)$.

Therefore, recalling that we consider sufficiently confining potentials $U(x)$, there exist a spectral expansion of the Fokker–Planck operator $\mathcal{L}_{\mathrm{FP}}$ with discrete eigenvalues $-\lambda_k \leqslant 0$ for $k = 0, 1, \ldots$ and corresponding symmetrized nontrivial solutions $\psi_k(x)$ to the eigenequation $\mathcal{L}_{\mathrm{FP}}\psi_k(x) = -\lambda_k\psi_k(x)$, which are assumed to be normalized $\int \psi_k(x)^2/P^{\mathrm{eq}}(x)\mathrm{d}x \equiv 1$. The ground state ψ_0 corresponding to eigenvalue $\lambda_0 = 0$ represents the equilibrium Boltzmann distribution $P^{\mathrm{eq}}(x) = \psi_0(x)$. Using the eigenfunctions $\{\psi_k\}$ and eigenvalues $\{\lambda_k\}$ defined this way, the Laplace transform of the ensemble propagator can be written in the form

$$\tilde{P}(a,s|x_0) = \frac{P^{\mathrm{eq}}(a)}{s} + \sum_{k=1}^{\infty} \frac{\psi_k(a)\psi_k(x_0)/P^{\mathrm{eq}}(x_0)}{s+\lambda_k}, \tag{12}$$

where $\psi_k(x)/P^{\mathrm{eq}}(x) \equiv \psi_k^\dagger(x)$ are in fact the eigenfunctions to the adjoint of $\mathcal{L}_{\mathrm{FP}}$, that is $\mathcal{L}_{\mathrm{FP}}^\dagger\psi^\dagger(x) = -\lambda_k\psi^\dagger(x)$. Note that in our previous work we used the equivalent non-symmetric eigenspectrum with right and left eigenfunctions ψ_k and $\psi_k^\dagger$, respectively [38, 39, 43]. Since the Laplace transform of a function f with a simple pole $\tilde{f}(s) = (s+\lambda)^{-1}$ yields in the time domain an exponentially decaying function $f(t) = \mathrm{e}^{-\lambda t}$ with rate λ, we can interpret the eigenvalues λ_k as relaxation rates, which characterize the speed at which the dynamics governed by equation (2) approaches the equilibrium $P^{\mathrm{eq}}(x) \propto \mathrm{e}^{-U(x)}$.

The Laplace transform of the first passage time density $\tilde{\wp}_a(s|x_0)$, as well has simple poles, which are located at $s = -\mu_k$ ($k = 1, 2, \ldots$) and need to be determined for equation (10) to be written as [38]

$$\tilde{\wp}_a(s|x_0) = \sum_{k=1}^{\infty} \frac{w_k(a,x_0)\mu_k(a)}{\mu_k + s}. \tag{13}$$

The expansion in equation (13) can formally be found by determining the zeros $s = -\mu_k$ that solve $\tilde{P}(a,s|a) = 0$, to which we refer as first passage rates μ_k. Determining all first passage rates μ_k, while doable in general, is rather involved and is described in [38, 39], whereas detailed information on the determination of slowest rate μ_1, to which we refer to as large deviation limit, can be found in section 2.3 below as well as in [44]. If all first passage rates $\{\mu_k\}$ are known, we can obtain the corresponding weights $w_k(a,x_0)$ in equation (13) directly from equation (10) using Cauchy's residue theorem

[2] The Laplace transform of a function $f(t)$ is defined by $\tilde{f}(s) = \int_0^\infty f(t)\mathrm{e}^{-st}\mathrm{d}t$.

$$w_k(a,x_0)\mu_k(a) = \left.\frac{\tilde{P}(a,s|x_0)}{\partial_s \tilde{P}(a,s|a)}\right|_{s=-\mu_k}. \tag{14}$$

Dividing equation (14) by $\mu_k(a)$ yields the 'weights' $w_k(a,x_0)$, which according to equation (13) are normalized such that $\tilde{\wp}_a(0|x_0) = \sum_k w_k(a,x_0) = 1$. Equation (13) in turn immediately yields the first passage time density

$$\wp_a(t|x_0) = \sum_{k>0} w_k(a,x_0)\mu_k(a)\mathrm{e}^{-\mu_k(a)t}, \tag{15}$$

and the corresponding survival probability

$$\mathcal{P}_a(t|x_0) = \int_t^\infty \wp_a(\tau|x_0)\mathrm{d}\tau = \sum_{k>0} w_k(a,x_0)\mathrm{e}^{-\mu_k(a)t}, \tag{16}$$

where we used equations (6) and (15). Inserting equations (16) into (7) allows us to rewrite the probability density of the extremum to have value a at time t as

$$p^\kappa(a|t,x_0) = \left|\partial_a P^\kappa(a|t,x_0)\right| = \left|\partial_a \mathcal{P}_a(t|x_0)\right| = \left|\sum_{k>0} \partial_a\left[w_k(a,x_0)\mathrm{e}^{-\mu_k(a)t}\right]\right|, \tag{17}$$

where $\kappa = \max$ or $\kappa = \min$.

2.3. Large deviation limit

At long times the extremum ($\overline{m}_t$ or $\underline{m}_t$) will be dominated by extreme fluctuations of the process x_t that are not reflected by the 'typical' equilibrium measure given by $P^{\mathrm{eq}}(x) \propto \mathrm{e}^{-U(x)}$. As a result, the extreme value distribution may differ substantially from the equilibrium Boltzmann distribution $P^{\mathrm{eq}}(x)$. Fortunately, at long times the first passage distribution will be dominated solely by the slowest first passage time-scale $1/\mu_1(a)$, which leads to what we refer here to as the *large deviation limit* that reads

$$p^\kappa_{\mathrm{LD}}(a|t,x_0) \equiv \left|\partial_a w_1(a,x_0)\mathrm{e}^{-\mu_1(a)t}\right| \simeq p^\kappa(a|t,x_0), \tag{18}$$

where '$\simeq$' denotes the asymptotic equality in the limit $t\to\infty$ and $\kappa = \max, \min$. An explicit general method to determine $w_1(a,x_0)$ and $\mu_1(a)$ can be found in [38, 39, 44]. We note that the large deviation limit becomes exact in the long time limit $\mathrm{e}^{-\mu_1(a)t} \gg \mathrm{e}^{-\mu_2(a)t}$ as well as whenever $w_1(a,x_0) \gg |w_{k\geqslant 2}(a,x_0)|$ holds.

We recall that according to equation (13) each first passage rate, μ_k, is located at a simple pole (at $s=-\mu_k$) of $\tilde{\wp}_a(s|x_0)$, which according to equation (10), is also a root of $\tilde{P}(a,s|a)$. Hence, the large deviation limit 'μ_1' is characterized by the root ($s<0$) closest to the origin, $s=-\mu_1$, solving $\tilde{P}(a,s|a)=0$. In order to determine μ_1 exactly, we Taylor-expand the function

$$f(s) = s\tilde{P}(a,s|a) = \sum_{n\geqslant 0} \sigma_n s^n/n! \tag{19}$$

around $s=0$, where σ_n is the nth derivative of f with respect to s, which according to equation (12) holds for all s within the radius of convergence $|s|<\lambda_1$[3]. Note that $f(s) = s\tilde{P}(a,s|a)$

[3] The radius of convergence is limited by the pole of $f(s) = s\tilde{P}(a,s|a)$ which is closest to the origin. According to equation (12) the closest pole to $s=0$ is located at $s=-\lambda_1$, yielding a converging sum equation (19) for all $|s|<\lambda_1$.

has the same non-trivial roots but, in contrast to $\tilde{P}(a,s|a)$, does not have a pole at the origin (see equation (12)), which is why we are always allowed to expand f as in equation (19). The closest non-trivial zero $s=-\mu_1$ with $0<\mu_1\leqslant\lambda_1$ can then be formally be found by a Newton's iteration, which in terms of a series of almost triangular matrices reads explicitly [39] (see also [38, 44])

$$\mu_1(a)=\sum_{n=1}^{\infty}\frac{\sigma_0^n}{\sigma_1^{2n-1}}\frac{\det\boldsymbol{\mathcal{A}}_n}{(n-1)} \tag{20}$$

where $\boldsymbol{\mathcal{A}}_n$ is a $(n-1)\times(n-1)$ almost triangular matrix with elements $(i,j=1,\ldots,n-1)$

$$\mathcal{A}_n^{ij}\equiv\frac{\sigma_{i-j+2}\Theta(i-j+1)}{(i-j+2)!}\times\begin{cases} i & \text{if } j=1,\\ n(i-j+1)+j-1 & \text{if } j>1,\end{cases} \tag{21}$$

with $\Theta(l)=1$ if $l\geqslant 0$ and $\Theta(l)=0$ if $l<0$ as well as $\det\boldsymbol{\mathcal{A}}_1\equiv 1$. Equation (20) exactly determines the first non-trivial root, $f(s)=0$ with $s=-\mu_1$, at which the right hand side of equation (19) vanishes. It should be noted that determining μ_1 in equation (20) requires only $\tilde{P}(a,s|a)$ or the coefficients σ_n from equation (19), whereas the expansion equation (12) including the eigenvalues $\{\lambda_k\}$ is generally not required to be known. The weight $w_1(a)$ can then be deduced from Cauchy's residue theorem equation (14)

$$w_1(a)=\left.\frac{\tilde{P}(a,-\mu_1(a)|x_0)}{\mu_1(a)\partial_s\tilde{P}(a,s|a)}\right|_{s=-\mu_1(a)}. \tag{22}$$

Equation (18) with equations (20) and (22) fully characterize the large deviation limit of the density of the extreme value $p_{\mathrm{LD}}^{\max}(a|x_0)$.

2.4. Large deviation limit in the presence of a spectral gap

In the large time limit the probability mass of the extremum $p^{\max}(a|t,x_0)$ or $p^{\min}(a|t,x_0)$ concentrates at the potential boundaries (i.e. $U(a)\gg k_{\mathrm{B}}T$), such that we can accurately approximate μ_1 by truncating equation (20) already after the first term yielding (see [38] for more details)

$$\tilde{\mu}_1(a)\equiv\frac{\sigma_0}{\sigma_1}\approx\mu_1(a), \tag{23}$$

where using equation (12) we can identify

$$\sigma_0=P^{\mathrm{eq}}(a)\qquad\text{and}\qquad\sigma_1=\int_0^{\infty}[P(a,t|a)-P^{\mathrm{eq}}(a)]\mathrm{d}t. \tag{24}$$

Since $f(s)\equiv s\tilde{P}(a,s|x_0)=\sigma_0+\sigma_1 s+\mathrm{O}(s)^2$, we expect equation (23) to be quite accurate as soon as the formal condition $\tilde{\mu}_1\ll\lambda_1$ is met, where λ_1 from equation (12) is the slowest rate at which the system approaches the equilibrium density [38]. Note that λ_1 in fact does not need to be known, as equation (23) necessarily becomes accurate at sufficiently high potential values $U(a)$, such that a is not located in the deepest point in the potential [38]. This also follows from the work of Matkowsky and Schuss, who have shown that λ_1 is the expected time to overcome the barriers on the way to the deepest potential well [45].

In fact, at very long times $t\to\infty$ the probability mass $p^{\kappa}(a|t,x_0)\simeq p_{\mathrm{LD}}^{\kappa}(a|t,x_0)$ (with $\kappa=\max,\min$) will inevitably be pushed towards the boundaries with high potential values, which will again render equation (23) asymptotically exact in the limit $U(a)\to\infty$. To prove

that equation (23) indeed becomes asymptotically exact, we inspect equation (12) in the following way. First, we find that $f(s) = s\tilde{P}(a,s|a)$ is a concave function $f''(s) \leqslant 0$ within the interval $-\lambda_1 \leqslant s \leqslant 0$, whereas $g(s) \equiv s(s+\lambda_1)\tilde{P}(a,s|a) = (s+\lambda_1)f(s)$ is a convex function $g''(s) \geqslant 0$ in the same interval. Hence, we find that the tangent $t_f(s) = \sigma_0 + s\sigma_1$ to f and the tangent $t_g(s) = \lambda_1\sigma_0 + (\sigma_0 + \lambda_1\sigma_1)s$ to g have roots that sandwich $s = -\mu_1$ according to

$$\frac{\tilde{\mu}_1(a)}{1+\tilde{\mu}_1(a)/\lambda_1} = \frac{\lambda_1\sigma_0}{\sigma_0+\lambda_1\sigma_1} \leqslant \mu_1(a) \leqslant \frac{\sigma_0}{\sigma_1} = \tilde{\mu}_1(a), \tag{25}$$

where the lower bound, $s = -\tilde{\mu}_1(1+\tilde{\mu}_1/\lambda_1)^{-1}$, solves $t_g(s) = 0$ and the upper bound, $s = -\tilde{\mu}_1$, solves $t_f(s) = 0$. The chain of inequalities equation (25) and its implications, which we explore below, are the main result of this paper. Notably, in the limit of $U(a) \gg k_\mathrm{B}T$, where $\tilde{\mu}_1 \to 0$ (i.e. $\tilde{\mu}_1 \ll \lambda_1$ [45]) holds, the inequalities in equation (25) saturate and provide an asymptotically exact value for μ_1.

We emphasize that the chain of inequalities (25) holds for the slowest time-scale μ_1^{-1} of the first passage process as well as for the slowest time-scale of the extremum functional, i.e. either the maximum or the minimum. For example, if $\mu_1^{\min}(a)$ and $\mu_1^{\max}(a)$ denote the large deviation limit of the minimum and maximum, respectively, then the slowest first passage rate is given by $\mu_1(a) = \min[\mu_1^{\max}(a), \mu_1^{\min}(a)]$. Since the maximum $\overline{m}_t = a \geqslant x_0$ after a long time t will be more likely located at the 'right' border of a confining potential, where $U(\overline{m}_t) \gg U(x_0)$, whereas the minimum $\underline{m}_t = a \leqslant x_0$ will more likely move to the 'left' border, where $U(\underline{m}_t) \gg U(x_0)$, we will use equation (25) to determine the minimum near the left boundary $a < x_0$ and to determine the maximum if $a > x_0$ is closer to the right boundary.

To be more specific, we use $\tilde{\mu}_1(a) \simeq \mu_1^{\max}(a)$ self-consistently for the large deviation limit of the maximum, whenever $\tilde{\mu}_1(a) \searrow$ is monotonically decreasing with increasing $a \nearrow$, whereas we use $\tilde{\mu}_1(a) \simeq \mu_1^{\min}(a)$ for the large deviation limit of the minimum, whenever $\tilde{\mu}_1(a) \searrow$ is monotonically decreasing with decreasing $a \searrow$. Notably, if a is located at a reflecting boundary, where formally $U(x) = \infty$ for $x \leqslant a$, we immediately get $\mu_1(a) = \mu_1^{\min}(a)$ and $\mu_1^{\max}(a) = \infty$, since for any $x_0 > a$ the maximum $\overline{m}_t$ cannot reach any value below x_0 and hence a certainly cannot correspond to the maximum[4].

3. Examples

3.1. Statistics of maxima in the Ornstein–Uhlenbeck process

As our first example we consider the Ornstein–Uhlenbeck process with $U(x) = x^2/2$. The corresponding propagator in the time domain is well known and reads [40]

$$P(a,t|x_0) = \frac{1}{\sqrt{2\pi(1-\mathrm{e}^{-2t})}} \exp\left[-\frac{(a-x_0\mathrm{e}^{-t})^2}{2(1-\mathrm{e}^{-2t})}\right] \tag{26}$$

with a Gaussian equilibrium density $P^{\mathrm{eq}}(a) = P(a,\infty|x_0) = (2\pi)^{-1/2}\exp(-a^2/2)$. Inserting equations (26) into (23) yields for $a \geqslant 0$ the following approximation for the large deviation eigenvalue of the density of the maximum[5]

[4] A similar finding can be found in [39], where $\mu_1(a) = \mu_1^{\min}(a)$ corresponds to a first passage to a, entering from the right, and $\mu_1(a) = \mu_1^{\max}(a)$ corresponds to a first passage to a, entering from the left. For example, if a reflecting boundary is located at a with $U(x) = \infty$ for $x \leqslant a$, it is impossible to enter a from the left.

[5] For $a \leqslant 0$ equation (27) approximates the large deviation limit of the minimum functional.

$$\tilde{\mu}_1(a) = \int_0^\infty \left[\frac{1}{\sqrt{1-\mathrm{e}^{-2t}}}\exp\left(\frac{a^2\mathrm{e}^{-t}}{1+\mathrm{e}^{-t}}\right) - 1\right]\mathrm{d}t \simeq \mu_1(a). \tag{27}$$

The relaxation eigenvalues are integers $\lambda_k = k$ with $k = 0, 1, \ldots$, such that equation (25) translates into

$$\tilde{\mu}_1(1+\tilde{\mu}_1)^{-1} \leqslant \mu_1 \leqslant \tilde{\mu}_1, \tag{28}$$

where the upper limit $\tilde{\mu}_1$ is depicted in figure 2(a) as the dash-dotted red line, the lower limit $\tilde{\mu}_1(1+\tilde{\mu}_1)^{-1}$ as the dashed green line, and the exact value μ_1, determined as described below, is given by the solid blue line. The inset displays the same results but scaled by the exact value μ_1. We emphasize that it is not necessary to determine μ_1 in order to show that equation (27) asymptotically saturates when $\tilde{\mu}_1$ approaches zero in the limit of large a, since $\tilde{\mu}_1 \simeq \mu_1$ follows immediately from $\tilde{\mu}_1(1+\tilde{\mu}_1)^{-1} \simeq \tilde{\mu}_1$ (for $\tilde{\mu}_1 \to 0$) as well as from equation (28). For completeness, we also present in figure 2(a) (dotted line) the long time asymptotics, $\mu_1 \simeq (2\pi)^{-1/2} a \mathrm{e}^{-a^2/2}$, for the limit $a \to \infty$, which have been reported previously [44, 46, 47].

In order to determine the large deviation eigenvalue μ_1 and weight w_1 entering $p_{\mathrm{LD}}^{\max}(a|t,x_0) = \partial_a w_1(a,x_0)\mathrm{e}^{-\mu_1(a)t}$, we Laplace-transform the propagator (26) in time ($t \to s$), which for $x_0 \leqslant a$ yields (see also [42])

$$\tilde{P}(a,s|x_0) = \Gamma(s)2^s P^{\mathrm{eq}}(a) H_{-s}(-a/\sqrt{2})H_{-s}(x_0/\sqrt{2}), \tag{29}$$

where $\Gamma(s)$ is the complex gamma function and $H_s(y)$ is the generalized Hermite polynomial. Inserting equation (29) into the renewal theorem (10) yields [42, 49, 50]

$$\tilde{\wp}_a(s|x_0) = \frac{H_{-s}(-x_0/\sqrt{2})}{H_{-s}(-a/\sqrt{2})}, \tag{30}$$

where $s = -\mu_1$ is the root, $H_{-s}(-a/\sqrt{2}) = 0$, closest to the origin such that the weight in equation (22) becomes [46, 48]

$$w_1(a) = -\frac{H_{\mu_1}(-x_0/\sqrt{2})}{\mu_1 h_{\mu_1}(-a/\sqrt{2})}, \tag{31}$$

where we introduced $h_s(y) \equiv \partial_s H_s(y)$. For convenience we determined μ_1 and w_1 numerically according to [48][6]. The results in figure 2(a) confirm the validity of the chain of inequalities in equation (25), which, as already mentioned, become asymptotically tight in the limit of high values of the potential, $U(a) = a^2/2 \gg 1$.

The lines in figure 2(b) represent the large deviation limit of the density of the maximum $p_{\mathrm{LD}}^{\max}(a|x_0) = \partial_a w_1(a,x_0)\mathrm{e}^{-\mu_1(a)t}$, which agree rather well with the density of the maximum $p^{\max}(a|x_0)$ (symbols) obtained from Brownian dynamic simulations with a time step $\mathrm{d}t = 10^{-5}$ using 10^5 trajectories.

We note that the large deviation limit $p_{\mathrm{LD}}^{\max}$ (see lines in figure 2(b)) approximates the density of the maximum $p^{\max}$ quite well already on relatively short time-scales $t \sim \lambda_1^{-1} = 1$ (see

[6] We note that with the eigenfunctions $\psi_k(a) = P^{\mathrm{eq}}(a)(k!2^k)^{-1/2}H_k(a/\sqrt{2})$ (see, e.g. [40]) and equations (12) and (19) we can formally identify

$$\sigma_0 = P^{\mathrm{eq}}(a) \qquad \text{and} \qquad \frac{\sigma_n}{n!} = P^{\mathrm{eq}}(a)(-1)^{n+1}\sum_{k=1}^{\infty}\frac{H_k(a/\sqrt{2})^2}{k!2^k k^n}, \tag{32}$$

which with equation (20) would be an alternative but equivalent approach for determining μ_1 as done, e.g. in [39].

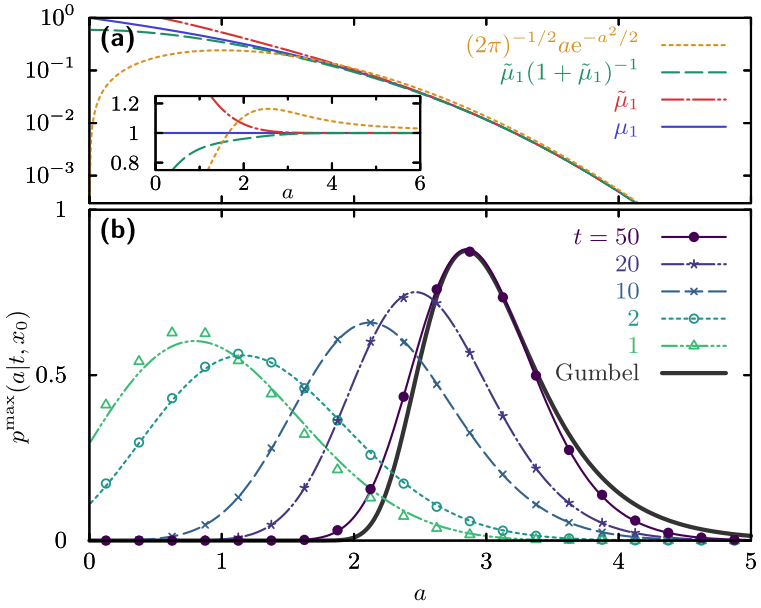

Figure 2. Probability density of the maximum and its large deviation limit for the Ornstein–Uhlenbeck process. (a) Large deviation eigenvalue $\mu_1(a)$ (solid blue line) compared to the approximation from equation (27) (dash-dotted red line) and the lower bound equation (25) (dashed green line); the dotted line represents the asymptotic approximation $(2\pi)^{-1/2}a\mathrm{e}^{-a^2/2} \simeq \mu_1(a)$ from, e.g. [44, 46, 47]. The inset shows the same result but scaled by μ_1, which was determined numerically by the root, $s\tilde{P}(a,s|a) = 0$, closest to the origin $s = -\mu_1$ (see, e.g. [48]). (b) Probability densities of the maximum $p^{\max}(a|t,x_0)$ (symbols) are obtained from simulating 10^5 trajectories for each time $t = 1, 2, 10, 20, 50$; the lines represent the large deviation limit $p^{\max}_{\mathrm{LD}}(a|t,x_0) = \partial_a w_1(a,x_0)\mathrm{e}^{-\mu_1(a)t}$, where μ_1 adopted from the upper panel (a) and w_1 is determined from equation (31). The thick gray line represents the Gumbel density $g(a,\eta,\gamma) = \gamma^{-1}\mathrm{e}^{-(a-\eta)/\gamma}\exp[-\mathrm{e}^{-(a-\eta)/\gamma}]$ with arbitrarily chosen parameters $\eta = 2.85$ and $\gamma = 0.42$ [16]. The initial condition was $x_0 = 0$ and the symbols are obtained from Brownian dynamics simulations with a time increment $\mathrm{d}t = 10^{-5}$.

triangles and dash-dotted light green line), where λ_1^{-1} represents the equilibration time of the Ornstein–Uhlenbeck process. Notably, even for long times (see, e.g. $t = 50$ in figure 2(b)), the left and right tails of the density of the maximum remain asymmetric yet still deviating from a Gumbel distribution [16] (see thick gray line in figure 2(b)). This indicates that the extreme value theorem for sequences of uncorrelated random variables becomes valid on much longer time-scales. Therefore, the large deviation limit presented here allows us to approximate extreme value statistics exceptionally well despite the fact that the extreme value theorem does not yet apply[7].

[7] We find that the probability density of the maximum approaches a Gumbel density on extremely large time-scales $t \gtrsim 10^3$. The underlying assumptions are the approximation $\mu_1 \simeq a(2\pi)^{-1/2}\mathrm{e}^{-a^2/2}$ (see inset of figure 2(a) for deviations) and $w_1 \simeq 1$ (which holds for $a \gtrsim 3$).

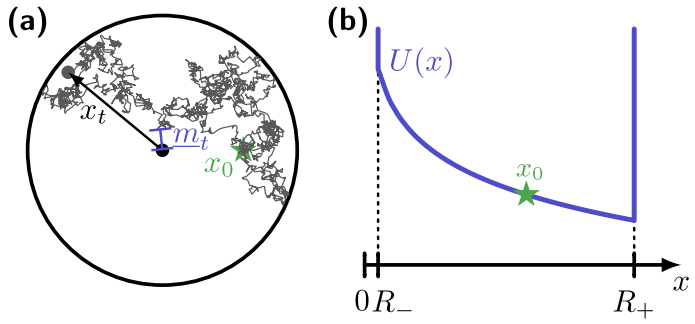

Figure 3. Graphical illustration of the Bessel process. (a) Trajectory of a Brownian motion starting from x_0 and ending at distance x_t after time t in $d = 2$ dimensions. The minimum of the distance is indicated as $\underline{m}_t$. (b) Effective potential $U(x) = -\ln(x^{d-1})$, where x denotes the distance to the origin and R_- the inner radius of the confinement and R_+ the outer radius of the volume.

3.2. Density of the minimum of the confined Bessel process

In our second example we consider the minimal distance to the origin of Brownian motion inside a d-dimensional sphere with inner radius $R_- \geqslant 0$ and a reflecting boundary at $R_+ < \infty$ (see figure 3(a) for an illustration with $R_- = 0$ and $d = 2$). The distance from the origin x_t (i.e. the radius) at time t within the interval $R_- \leqslant x \leqslant R_+$ obeys the Langevin equation

$$\dot{x}_t = \frac{d-1}{x_t} + \xi_t \tag{33}$$

where $\langle \xi_t \rangle$ and $\langle \xi_t \xi_{t'} \rangle = 2\delta(t - t')$. This process is also known as the Bessel process [51, 52]. We note that the maximum excursion of the free Bessel process (see e.g. [53]), which in the present context corresponds to the limiting case with $R_+ = \infty$ and will not be considered here, allows in the specific case of $d = 3$ a mapping onto a simpler problem for the 1-dimensional Brownian motion [51].

Comparing equations (1) and (33) allows us to identify the geometric free energy $U(x) = -(d-1)\ln x$ of purely entropic origin and accounts for the invariance with respect to angular degrees of freedom $\propto x^{d-1}$ (see figure 3(b)). The equilibrium measure corresponds to a uniform distribution in a d-dimensional hyperspherical shell and is given by $P^{\mathrm{eq}}(x) = \mathrm{d}x^{d-1}/(R_+^d - R_-^d)$.

For simplicity we here from restrict our discussion to the case $d = 3$, yielding the Fokker–Planck equation

$$\frac{\partial}{\partial t} P(x,t|x_0) = \left[\frac{\partial^2}{\partial x^2} - \frac{\partial}{\partial x} \frac{2}{x} \right] P(x,t|x_0) \tag{34}$$

with zero flux boundary condition $J(R_\pm, t|x_0) = 0$, where $J(x,t|x_0) \equiv (2/x - \partial_x) P(x,t|x_0)$. We emphasize that the probability density P is normalized according to $\int_{R_-}^{R_+} P(x,t|x_0)\mathrm{d}x = 1$, whereas the radial density, discussed for example in [54], would correspond to $P(x,t|x_0)/(4\pi x^2)$ instead. A Laplace transform in t yields

$$\left[\frac{\partial^2}{\partial x^2} - \frac{\partial}{\partial x} \frac{2}{x} - s \right] \tilde{P}(x,s|x_0) = -\delta(x - x_0), \tag{35}$$

where the solution $\tilde{P}(x,s|x_0)$ can be constructed from the two solutions of the homogeneous problem, $v_1(x,s) = x\mathrm{e}^{-x\sqrt{s}}$ and $v_2(x,s) = x\mathrm{e}^{x\sqrt{s}}/\sqrt{s}$ obtained by setting the right hand side of equation (35) to zero. The Laplace transform of the propagator for a Brownian particle confined between $R_- = a$ and $R_+ = R$ in turn reads

$$\tilde{P}(a,s|x_0) = \frac{a^2 \sinh\left[\sqrt{s}\,(R-x_0)\right] - a^2 R\sqrt{s}\cosh\left[\sqrt{s}\,(R-x_0)\right]}{x_0(1-aRs)\sinh\left[\sqrt{s}(R-a)\right] - \sqrt{s}x_0(R-a)\cosh\left[\sqrt{s}(R-a)\right]}. \tag{36}$$

We are allowed to choose $R_- = a$, since the first passage time distribution from x_0 to $a \leqslant x_0$ is not affected by the potential $U(x)$ in the region $x \leqslant a$, where $R_- = a$ formally corresponds to $U(x) = \infty$ for $x \leqslant a$ (see also the discussion at the end of section 2.1). Most importantly, setting $R_- = a$ removes all roots of $\tilde{P}(a,s|a)$, which would account for the maximum of the Bessel process. In other words, in the presence of a reflecting boundary at a every single root of $\tilde{P}(a,s|x_0{=}a)$ from equation (36) is indeed a first passage time scale for approaching a for the first time from above (for more details on the influence of boundary condition please see [39]). Moreover, the limit $R = R_+ = \infty$, which is not considered here, would allow us to map the 3d-Bessel process to 1d Brownian motion [51] with $\tilde{\wp}_a(s|x_0) = \tilde{P}(a,s|x_0)/\tilde{P}(a,s|a) \to (a/x_0)\exp[\sqrt{s}(a-x_0)]$, which would in turn yield the Lévy–Smirnov density[8].

For $R < \infty$, we use equation (36) to identify the Taylor coefficients of $s\tilde{P}(a,s|a)$, which we denote by σ_n according to equation (19). The exact smallest eigenvalue μ_1 is then determined using equation (20). The results are presented in figure 4(a) (see solid blue line), where we also compare μ_1 to the approximation $\tilde{\mu}_1$ from equation (23) (see dash-dotted red line), which for the $3d$-Bessel process reads

$$\tilde{\mu}_1(a) = \frac{\sigma_0}{\sigma_1} = \frac{15a\left(a^2+aR+R^2\right)}{(a-R)^2\left(a^3+3a^2R+6aR^2+5R^3\right)} \simeq \mu_1(a). \tag{37}$$

Equation (37) delivers the exact value for μ_1 in the limit $a \to 0$ as shown in figure 4(a), where the relative deviation $\epsilon \equiv (\tilde{\mu}_1 - \mu_1)/\mu_1$ vanishes in the limit $a \to 0$ (see dashed green line). It should be noted that μ_1, given by the series equation (20), is in fact an explicit solution of the transcendental equation $R\sqrt{\mu_1} = \tan[(R-a)\sqrt{\mu_1}]$ in the form of a Newton's series.

To rationalize why equation (37) becomes asymptotically exact as a approaches zero, we recall that $\lambda_1 \approx 0.81$ is the slowest relaxation rate corresponding to $R_- = 0$, which solves $R\sqrt{\lambda_1} = \tan(R\sqrt{\lambda_1})$ (here using $R = 5$). Since equation (36) obeys a reflecting boundary condition at a, we have that $\lambda_1(a) \geqslant \lambda_1 \approx 0.81$, i.e. the eigenvalue $\mu_1(a)$ is bounded by $\tilde{\mu}_1(1-\tilde{\mu}_1/0.81) \leqslant \mu_1 \leqslant \tilde{\mu}_1$. Hence for asymptotically high potentials (here $U(a) = -2\ln a \to \infty$ as $a \to 0$) the inequality equation (25) renders $\tilde{\mu}_1$ asymptotically exact as soon as $\tilde{\mu}_1(a)/0.81 \to 0$.

In figure 4(b) we compare the density of the minimum $p^{\min}$ (symbols), obtained from simulations of 10^5 trajectories (with $R_- = 0$, $R_+ = R = 5$ and starting condition $x_0 = 3$), to the corresponding large deviation limit $p^{\min}_{\mathrm{LD}}(a|t,x_0) = -\partial_a w_1(a,x_0)\mathrm{e}^{-\mu_1(a)t}$ (lines), where we determined w_1 using equation (22) and took the exact $\mu_1(a)$ obtained using equation (36). The error bars in the simulation results denote 95% confidence intervals.

By design the large deviation limit $p^{\min}_{\mathrm{LD}}$ approaches the density of the minimum $p^{\min}$ in the long time limit, which is perfectly corroborated by simulation results for $t = 40$ ($\gg \lambda_1^{-1} \approx 1.2$)

[8] The Lévy–Smirnov density is defined as $\wp_a(t|x_0) = (a/x_0) \times (x_0-a)/\sqrt{4\pi t^3} \times \mathrm{e}^{-(x_0-a)^2/(4t)}$.

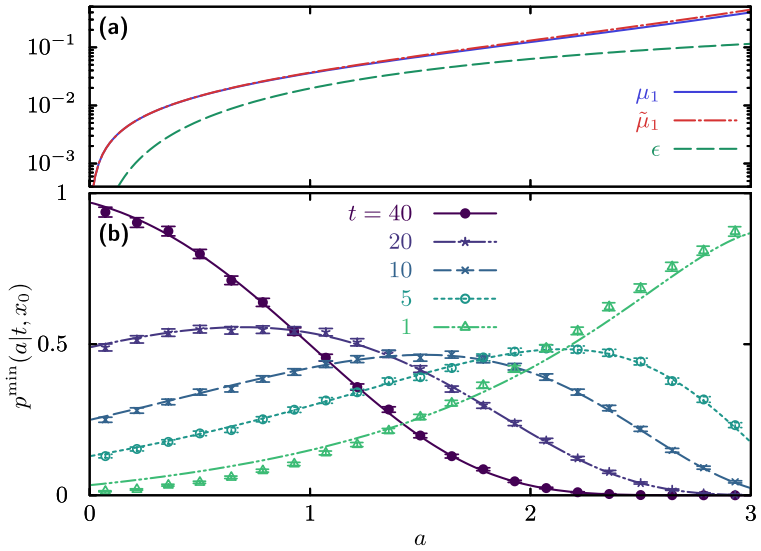

Figure 4. Probability density of the minimum of a 3d Bessel process. (a) Slowest time scale μ_1 (solid blue line) and its approximation $\tilde{\mu}_1$ (dash-dotted red line) given by equation (37) as a function function of the distance to the origin a; we truncated equation (20) after $n = 10$ to calculate μ_1. The corresponding relative deviation $\epsilon(a) = [\tilde{\mu}_1(a) - \mu_1(a)]/\mu_1(a)$ is depicted by the dashed green line. (b) Probability density of the minimum (symbols), $p^{\min}(a|t, x_0)$, sampled from 10^5 Brownian trajectories obtained by evolving equation (33) with time increment $\mathrm{d}t = 10^{-5}$ and using $R_- = 0$; error-bars indicate 95% confidence intervals. The large deviation limit $p^{\min}_{\mathrm{LD}}(a|t, x_0) = -\partial_a w_1(a, x_0)\mathrm{e}^{-\mu_1(a)t}$ (lines) determined using the eigenvalues $\mu_1(a)$ from (a) and the weight w_1 from equations (22) and (36). All results correspond to an initial distance $x_0 = 3$ and an outer radius $R_+ = 5$.

in figure 4(b). Notably, $p^{\min}_{\mathrm{LD}}$ (see solid dark-blue line in figure 4(b)) approximates quite well the full probability density of the minimum $p^{\min}$ (see filled circles).

To our surprise, the large deviation limit $p^{\min}_{\mathrm{LD}}$ can approximate $p^{\min}$ even for smaller times (e.g. $t = 1$), i.e. those that are shorter than the equilibration time $\lambda_1^{-1} \approx 1.2$ (see dash-dotted green line versus open triangles), which can be explained as follows. For any a within $0 \leqslant a \leqslant 3 = x_0$ we find a spectral gap $\mu_1(a) \ll \mu_2(a)$, which for $1.5 \lesssim a \leqslant 3$ also satisfies $\mu_2(a) \gg \lambda_1(a) \approx 0.81$. This in turn implies that for $t = 1 \sim \lambda_1^{-1}$ the condition $\mathrm{e}^{-\mu_1 t} \gg \mathrm{e}^{-\mu_2 t}$ is still met, whereas the relative deviations between $p^{\min}$ and $p^{\min}_{\mathrm{LD}}$ (i.e. between the open triangles and the dash-dotted green line) become substantial for small values of a (see $a \leqslant 1$) and $\mu_2(a)$ concurrently approaches $\lambda_1 \simeq 0.8$. Once the time exceeds $\lambda_1 t \approx 0.81t \gg 1$, the condition $\mathrm{e}^{-\mu_1 t} \gg \mathrm{e}^{-\mu_2 t}$ is satisfied for any value of a, and thus $p^{\min}_{\mathrm{LD}}$ approximates $p^{\min}$ over the full range (see symbols and lines in figure 4(b) for $t \geqslant 5$). Therefore, $p^{\min}_{\mathrm{LD}}$ approximates $p^{\min}$ rather well for any value a and on all time scales longer than the equilibration time scale ($t \gg \lambda_1^{-1}$).

Let us finally discuss the 'ultimate' long time limit ($t \to \infty$) in which the density of the minimum $p^{\min}(a|t, x_0)$ will be sharply peaked around the shortest distance $a = 0$. Inspecting equation (37) one can easily find $\mu_1(a) = 3a/R^3 + \mathrm{O}(a)$. Moreover, at high values of the potential the weight becomes $w_1(a, x_0) = 1 + \mathrm{O}(a)$ implying that the limiting density becomes $p^{\min}(a|t, x_0) \to 3tR^{-3}\mathrm{e}^{-3at/R^3}$, which is an exponential distribution falling into the

class of Weibull distributions. At $t = 40$ (see figure 4(b)) the density of the minimum still qualitatively deviates from an exponential density; while the exponential density is a convex function of a the resulting curve from figure 4(b) for $t = 40$ clearly did not yet reach a convex shape in a. While the Ornstein–Uhlenbeck process shows a Gumbel distribution in the limit $t \to \infty$, the Bessel process provides an example in which the extreme value distribution falls into the class of Weibull distributions.

4. Concluding perspectives

We used the link between first passage and extremum functionals of reversible ergodic Markov processes in order to formulate the probability density of extreme values in terms of the first passage times. We pushed the connection between these two functionals even further, by utilizing the duality between first passage and relaxation processes [38, 39], which allowed us to determine the statistics of extremes from transition probability densities describing the relaxation towards equilibrium. In their present form our results hold for diffusion in effectively one-dimensional potential landscapes that are sufficiently confining to allow for a discrete eigenspectrum of the corresponding Fokker–Planck operator. Our findings provide a new and deeper perspective on the study of extrema of asymmetric diffusion processes beyond a constant drift. We emphasize that the full probability density of extreme values ($p^{\max}$ or $p^{\min}$) on arbitrary time-scales still requires the knowledge of the eigenspectrum of the Fokker–Planck operator.

To avoid an eigendecomposition of the Fokker–Planck operator entirely, we established the long time asymptotics of the distribution of extreme values, $p^{\max}_{\mathrm{LD}} \simeq p^{\max}_{\mathrm{LD}}$ (or $p^{\min}_{\mathrm{LD}} \simeq p^{\min}$), which accounts for the slowest decaying mode $\propto \mathrm{e}^{-\mu_1 t}$ ignoring all faster decaying contributions ($\propto \mathrm{e}^{-\mu_2 t}, \mathrm{e}^{-\mu_3 t}$, etc). In this large deviation limit we determined explicit bounds on the exact slowest time-scale μ_1^{-1}, and showed that these asymptotically tightly bound μ_1 from above and from below, which is the central result of this paper.

We illustrated the usefulness of our results by analyzing the statistics of maximum value of the Ornstein–Uhlenbeck process and the minimal distance to the origin of a confined 3d Brownian motion (Bessel process). Our examples underline that the large deviation limit, albeit designed to be asymptotically exact for infinitely long times, approximates the density of the maximum surprisingly well even on relatively short times comparable to the relaxation time, $t \gtrsim 1/\lambda_1$. Since $t = 1/\lambda_1$ reflects the time-scale on which the process tends to decorrelate from the initial condition, the present results describe the statistics of extrema in presence of weak but non-vanishing correlations, and hence go beyond the three classes of limit laws for non-correlated random variables, i.e. the Gumbel, Fréchet, and Weibull distributions [14, 16–20] as demonstrated on hand of the Ornstein–Uhlenbeck and Bessel process. More generally, it would be interesting to systematically investigate the effect of the potential shape on the limiting extreme value distribution as in [18].

The remarkable accuracy of the approximation can readily be explained by the interlacing of first passage and relaxation time-scales ($\mu_1 \leqslant \lambda_1 \leqslant \mu_2 \ldots$) [38, 39], which renders all higher contributions ($\propto \mathrm{e}^{-\mu_2 t}, \mathrm{e}^{-\mu_3 t} \ldots$) negligibly small compared to the large deviation limit $\propto \mathrm{e}^{-\mu_1 t}$ once the condition $t \gtrsim \lambda_1^{-1}$ is met.

Our results can be extended and generalized in various ways. Extending the formalism presented here to systems obeying a discrete state Master equation would be straightforward; for example, our main result equation (25) would still hold by formally replacing the probability densities from equation (24) by the corresponding state probabilities [39]. Interesting and challenging extensions could include the consideration of trapping times [55, 56], spatial

disorder [57] and multi-channel transport [58], as well as extreme value statistics in discrete-state Markov processes with a broken time-reversal symmetry [34, 35].

Acknowledgments

The financial support from the German Research Foundation (DFG) through the Emmy Noether Program 'GO 2762/1-1' (to AG) is gratefully acknowledged.

ORCID iDs

Aljaž Godec https://orcid.org/0000-0003-1888-6666

References

[1] Redner S and Petersen M R 2006 Role of global warming on the statistics of record-breaking temperatures *Phys. Rev.* E **74** 061114
[2] Wergen G and Krug J 2010 Record-breaking temperatures reveal a warming climate *Europhys. Lett.* **92** 30008
[3] Nadarajah S 2005 Extremes of daily rainfall in west central Florida *Clim. Change* **69** 325
[4] Majumdar S N, von Bomhard P and Krug J 2019 An exactly solvable record model for rainfall *Phys. Rev. Lett.* **122** 158702
[5] Coumou D and Rahmsdorf S 2012 A decade of weather extremes *Nat. Clim. Change* **2** 491
[6] Sornette D, Knopoff L, Kagan Y Y and Vanneste C 1996 Rank-ordering statistics of extreme events: application to the distribution of large earthquakes *J. Geophys. Res.* **101** 13883
[7] Embrechts P, Klüppelberg C and Mikosch T 1997 *Modelling Extremal Events (For Insurance and Finance)* (Berlin: Springer)
[8] Sabir B and Santhanam M S 2014 Record statistics of financial time series and geometric random walks *Phys. Rev.* E **90** 032126
[9] Gembris D, Taylor J G and Suter D 2002 Trends and random fluctuations in athletics *Nature* **417** 506
[10] Ben-Naim E, Redner S and Vazquez F 2007 Scaling in tournaments *Europhys. Lett.* **77** 30005
[11] Dean D S and Majumdar S N 2006 Large deviations of extreme eigenvalues of random matrices *Phys. Rev. Lett.* **97** 160201
[12] Dean D S and Majumdar S N 2008 Extreme value statistics of eigenvalues of Gaussian random matrices *Phys. Rev.* E **77** 041108
[13] Eliazar I, Metzler R and Reuveni S 2018 Universal max-min and min-max statistics (arXiv:1808.08423 [cond-mat.stat-mech])
[14] Wergen G 2013 Records in stochastic processes-theory and applications *J. Phys. A: Math. Theor.* **46** 223001
[15] Godrèche C, Majumdar S N and Schehr G 2017 Record statistics of a strongly correlated time series: random walks and Lévy flights *J. Phys. A: Math. Theor.* **50** 333001
[16] Gumbel E J 1958 *Statistics of Extremes* (New York: Columbia University Press)
[17] Bertin E and Clusel M 2006 Generalized extreme value statistics and sum of correlated variables *J. Phys. A: Math. Gen.* **39** 7607
[18] Sabhapandit S and Majumdar S N 2007 Density of near-extreme events *Phys. Rev. Lett.* **98** 140201
[19] Krug J 2007 Records in a changing world *J. Stat. Mech.* P07001
[20] Lucarini V, Faranda D and Wouters J 2012 Universal behaviour of extreme value statistics for selected observables of dynamical systems *J. Stat. Phys.* **147** 63
[21] Comtet A and Majumdar S N 2005 Precise asymptotics for a random walker's maximum *J. Stat. Mech.* P06013
[22] Majumdar S N and Ziff R M 2008 Universal record statistics of random walks and Lévy flights *Phys. Rev. Lett.* **101** 050601

[23] Majumdar S N 2010 Universal first-passage properties of discrete-time random walks and Lévy flights on a line: statistics of the global maximum and records *Physica* A **389** 4299
[24] Bénichou O, Krapivsky P L, Mejía-Monasterio C and Oshanin G 2016 Temporal correlations of the running maximum of a Brownian trajectory *Phys. Rev. Lett.* **117** 080601
[25] Bénichou O, Krapivsky P L, Mejía-Monasterio C and Oshanin G 2016 Joint distributions of partial and global maxima of a Brownian bridge *J. Phys. A: Math. Theor.* **49** 335002
[26] Godrèche C, Majumdar S N and Schehr G 2009 Longest excursion of stochastic processes in nonequilibrium systems *Phys. Rev. Lett.* **102** 240602
[27] Majumdar S N, Schehr G and Wergen G 2012 Record statistics and persistence for a random walk with a drift *J. Phys. A: Math. Theor.* **45** 355002
[28] Szabó R and Vető B 2016 Ages of records in random walks *J. Stat. Phys.* **165** 1086
[29] Edery Y, Kostinski A B, Majumdar S N and Berkowitz B 2013 Record-breaking statistics for random walks in the presence of measurement error and noise *Phys. Rev. Lett.* **110** 180602
[30] Wergen G, Bogner M and Krug J 2011 Record statistics for biased random walks, with an application to financial data *Phys. Rev.* E **83** 051109
[31] Martin R J and Kearney M J 2018 Time since maximum of Brownian motion and asymmetric Lévy processes *J. Phys. A: Math. Theor.* **51** 275001
[32] Mounaix P, Majumdar S N and Schehr G 2018 Asymptotics for the expected maximum of random walks and Lévy flights with a constant drift *J. Stat. Mech.* 083201
[33] Kindermann F, Hohmann M, Lausch T, Mayer D, Schmidt F and Widera A 2017 Extreme event statistics in a drifting Markov chain *Phys. Rev.* E **96** 012130
[34] Neri I, Roldán É and Jülicher F 2017 Statistics of infima and stopping times of entropy production and applications to active molecular processes *Phys. Rev.* X **7** 011019
[35] Singh S, Roldán É, Neri I, Khaymovich I M, Golubev D S, Maisi V F, Peltonen J T, Jülicher F and Pekola J P 2019 Extreme reductions of entropy in an electronic double dot *Phys. Rev.* B **99** 115422
[36] Bray A J, Majumdar S N and Schehr G 2013 Persistence and first-passage properties in nonequilibrium systems *Adv. Phys.* **62** 225
[37] Schehr G and Majumdar S N 2014 Exact record and order statistics of random walks via first-passage ideas *First-Passage Phenomena and their Applications* ed R Metzler *et al* (Singapore: World Scientific) ch 1, p 226
[38] Hartich D and Godec A 2018 Duality between relaxation and first passage in reversible Markov dynamics: rugged energy landscapes disentangled *New J. Phys.* **20** 112002
[39] Hartich D and Godec A 2019 Interlacing relaxation and first-passage phenomena in reversible discrete and continuous space Markovian dynamics *J. Stat. Mech.* 024002
[40] Gardiner C W 2004 *Handbook of Stochastic Methods* 3rd edn (Berlin: Springer)
[41] Coffman E G, Flajolet P, Flatto L and Hofri M 1998 The maximum of a random walk and its application to rectangle packing *Probab. Eng. Inf. Sci.* **12** 373
[42] Siegert A J F 1951 On the first passage time probability problem *Phys. Rev.* **81** 617
[43] Lapolla A and Godec A 2018 Unfolding tagged particle histories in single-file diffusion: exact single- and two-tag local times beyond large deviation theory *New J. Phys.* **20** 113021
[44] Godec A and Metzler R 2016 Universal proximity effect in target search kinetics in the few-encounter limit *Phys. Rev.* X **6** 041037
[45] Matkowsky B J and Schuss Z 1981 Eigenvalues of the Fokker–Planck operator and the approach to equilibrium for diffusions in potential fields *SIAM J. Appl. Math.* **40** 242
[46] Ricciardi L M and Sato S 1988 First-passage-time density and moments of the Ornstein–Uhlenbeck process *J. Appl. Probab.* **25** 43
[47] Majumdar S N and Pal A 2014 Extreme value statistics of correlated random variables (arXiv:1406.6768 [cond-mat.stat-mech])
[48] Alili L, Patie P and Pedersen J L 2005 Representations of the first hitting time density of an Ornstein–Uhlenbeck process' 2005 *Stoch. Models* **21** 967
[49] Margolin G and Barkai E 2005 Single-molecule chemical reactions: reexamination of the Kramers approach *Phys. Rev.* E **72** 025101
[50] Martin R J, Kearney M J and Craster R V 2019 Long- and short-time asymptotics of the first-passage time of the Ornstein–Uhlenbeck and other mean-reverting processes *J. Phys. A: Math. Theor.* **52** 134001
[51] Pitman J W 1975 One-dimensional Brownian motion and the three-dimensional Bessel process *Adv. Appl. Probab.* **7** 511

[52] Barkai E, Aghion E and Kessler D A 2014 From the area under the Bessel excursion to anomalous diffusion of cold atoms *Phys. Rev.* X **4** 021036
[53] Schehr G and Le Doussal P 2010 Extreme value statistics from the real space renormalization group: Brownian motion, Bessel processes and continuous time random walks *J. Stat. Mech.* P01009
[54] Redner S 2001 *A Guide to First-Passage Processes* (Cambridge: Cambridge University Press)
[55] Condamin S, Bénichou O and Klafter J 2007 First-passage time distributions for subdiffusion in confined geometry *Phys. Rev. Lett.* **98** 250602
[56] Krüsemann H, Godec A and Metzler R 2014 First-passage statistics for aging diffusion in systems with annealed and quenched disorder *Phys. Rev.* E **89** 040101
[57] Godec A and Metzler R 2016 First passage time distribution in heterogeneity controlled kinetics: going beyond the mean first passage time *Sci. Rep.* **6** 20349
[58] Godec A and Metzler R 2017 First passage time statistics for two-channel diffusion *J. Phys. A: Math. Theor.* **50** 084001